

STUDY OF RIDE AND HANDLING IMPROVEMENT OF PICKUP LIGHT TRUCK VEHICLES USING ROBUST SEMI-ACTIVE SUSPENSION CONTROL BASED ON MAGNETO-RHEOLOGICAL DAMPERS

Claudio Crivellaro

DANA Structural Solutions International - Brazil Division (Dana Industrias Ltda)

e-mail: claudio.crivellaro@dana.com

Edilson Hiroshi Tamai

State University of São Paulo – UNESP-DEM

e-mail: edhtamai@usp.br

Abstract. *This work brings up two important results regarding suspension vehicle control. First, the kind of the system structure to be controlled has the peculiarity that the control input directly affects the output of the system, once we have the damper force as control actuator and body accelerations as measured variables. Thus a complete approach of LQG/LTR Robust Control design is needed to lead with this kind of control problem in order to guarantee the “Loop Transfer Recovery”, which is the heart of such technique. On the other hand we have the magnet-rheological device, which is able only to generate dissipative forces, i.e., this kind of component cannot generate all forces required by the control. However, it was possible to show through computer simulations the feasibility of semi-active implementation of LQG/LTR control in order to get ride performance improvement, although it was not as good as full active approach.*

Keywords. *Suspension, vehicle, Robust Control, LQG/LTR, Magneto-Rheological (MR) Damper.*

1. Introduction

Nowadays in the automotive industry, the sport utility vehicles are becoming more common and winning new markets day by day. In special light trucks as pickups have been used for people in big urban centers as well as people on the countryside. Sometimes pickups are used only for people locomotion, and in other times are used for load transportation, so they are a kind of vehicle that have bad features of ride and handling, because the passive suspension design can not overcome so different vehicle conditions: loaded or unload situations.

On the other hand, active suspensions can overcome many limitations of passive systems and eliminate, or at least decrease, the need to compromise among a variety of operating conditions and among the generally conflicting goals of providing good isolation of the body (ride comfort), maintaining uninterrupted contact between the tires and the road (road holding), and stabilizing the vehicle body (handling). They tend, however, to be expensive and as a result of their complexity, they may be unable to achieve the level of reliability typical for passive systems. Semi-active suspensions, which use adjustable dampers as force actuators (like magneto-rheological dampers), are a reasonable compromise between cost and performance. By varying the rate of energy dissipation, these suspensions can in principle generate forces that track those developed by active suspensions, as long as the required forces require dissipation of energy within the limits set for semi-active dampers.

The magneto-rheological dampers were considered in this work due to their characteristics of short response time (about 5ms) and low level of electric energy consume (around 20W), and also because they have already become such a commercial product.

The goal of this paper is to design a semi-active suspension using LQG/LTR robust control techniques and to demonstrate, by numeric simulation on a computer, the viability of this kind of suspension applied to pickup truck vehicles.

2. System Description

A two-dimensional four-degree-of-freedom half-car model is used in this study, as shown in Fig. (1). The cornering dynamics is not considered in this work. It is assumed that the tires do not leave the ground, all parameters are available under half vehicle assumption, the non-linearities of passive elements are neglected and the vehicle sprung mass is considered as a rigid body.

Notation:

- M_{AB} = half vehicle sprung mass. [516kg without load and 887kg with load];
- J_{AB} = pitch inertia of sprung mass. [990kg.m² without load and 2025kg.m² with load];
- m_{A1} = front unsprung mass. [50 kg];
- m_{B1} = rear unsprung mass (Part of differential axle considered). [80 kg];
- k_{A01} and k_{B01} = front and rear tire stiffness. [350 kN/m];
- b_{A01} and b_{B01} = front and rear tire damping. [300 Ns/m];
- k_{A12} =spring constant of front suspension. [30 kN/m];

k_{B12} = spring constant of rear suspension. [50 kN/m];
 b_{A12} =damping ratio of front suspension. [1750 Ns/m normal or 400 Ns/m in "soft-damping" mode];
 b_{B12} = damping ratio of rear suspension. [2250 Ns/m normal or 400 Ns/m in "soft-damping" mode];
 G = vehicle mass center;
 A = front suspension position;
 B = rear suspension position;
 M = driver position;
 l_A = distance from A point to G point. [1.115m without load and 1.780m with load];
 l_B = distance from B point to G point. [1.715m without load and 1.050m with load];
 g = gravity acceleration. [9.8 m/s²];

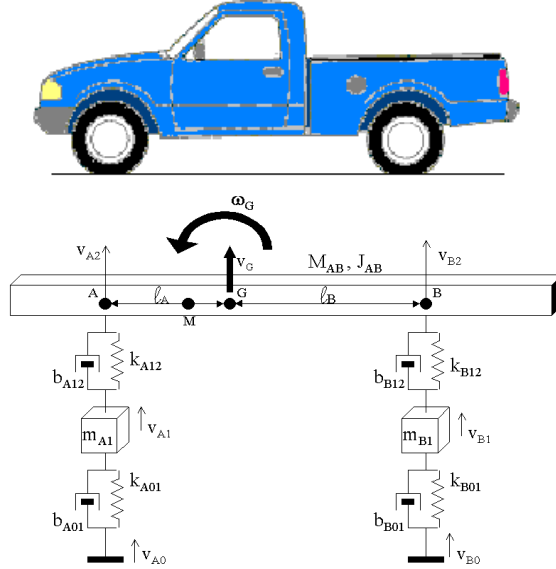


Figure 1. Vehicle Model.

The ride performance will be evaluated according to RMS value of vertical accelerations of sprung mass center and pitch acceleration of the body. Although the modeling assumptions used in this study largely simplify the real structure, they are commonly adopted in the literature (Hac' and Inman, 1996, Simon, 2002) and they include the most fundamental characteristics of the system behavior, what is enough for the conclusions which this work is proposed to achieve.

The control inputs are the forces f_A and f_B , which can represent active forces or semi-active and act as contraction or distension forces between sprung and unsprung masses.

The Bond Graph Techniques was used to generate the dynamic equations of the model (Eq. (1) to Eq. (6)); including the heavy and the pitch motions. The definitions used for some variables in the dynamic equations are shown in Eq. (7) e Eq. (8). The four equations on Eq. (8) are valid only because it was assumed that pitch angle is small (less than $\sim 14^\circ$), i.e., we can accept the following approximation: $\sin(x) \cong x$.

$$\ddot{x}_{A1} = \dot{v}_{A1} = \frac{1}{m_{A1}} [(k_{A01} \cdot x_{A01} + b_{A01} \cdot v_{A01}) - (k_{A12} \cdot x_{A12} + b_{A12} \cdot v_{A12})] - g \quad (1)$$

$$\ddot{x}_{B1} = \dot{v}_{B1} = \frac{1}{m_{B1}} [(k_{B01} \cdot x_{B01} + b_{B01} \cdot v_{B01}) - (k_{B12} \cdot x_{B12} + b_{B12} \cdot v_{B12})] - g \quad (2)$$

$$\ddot{\theta}_G = \dot{\omega}_G = \frac{1}{J_{AB}} [-(k_{A12} \cdot x_{A12} + b_{A12} \cdot v_{A12}) \cdot l_A + (k_{B12} \cdot x_{B12} + b_{B12} \cdot v_{B12}) \cdot l_B] \quad (3)$$

$$\ddot{x}_G = \dot{v}_G = \frac{1}{M_{AB}} [(k_{A12} \cdot x_{A12} + b_{A12} \cdot v_{A12}) + (k_{B12} \cdot x_{B12} + b_{B12} \cdot v_{B12})] - g \quad (4)$$

$$\frac{dx_{A01}}{dt} = \dot{x}_{A01} = v_{A01}; \frac{dx_{A12}}{dt} = \dot{x}_{A12} = v_{A12} \quad (5)$$

$$\frac{dx_{B01}}{dt} = \dot{x}_{B01} = v_{B01}; \frac{dx_{B12}}{dt} = \dot{x}_{B12} = v_{B12} \quad (6)$$

$$\left. \begin{aligned} x_{A12} &= x_{A1} - x_{A2}; v_{A12} = v_{A1} - v_{A2} \\ x_{B12} &= x_{B1} - x_{B2}; v_{B12} = v_{B1} - v_{B2} \\ x_{A01} &= x_{A0} - x_{A1}; v_{A01} = v_{A0} - v_{A1} \\ x_{B01} &= x_{B0} - x_{B1}; v_{B01} = v_{B0} - v_{B1} \end{aligned} \right\} \quad (7)$$

$$\left. \begin{aligned} x_{A2} &= x_G - \ell_A \cdot \theta_G; v_{A2} = v_G - \ell_A \cdot \omega_G \\ x_{B2} &= x_G + \ell_B \cdot \theta_G; v_{B2} = v_G + \ell_B \cdot \omega_G \end{aligned} \right\} \quad (8)$$

We can rewrite those equations on the space state form through some algebraic manipulation, and so represent it in the matrix notation shown in Eq. (9):

$$\begin{aligned} \dot{x}(t) &= A \cdot x(t) + B_1 \cdot w(t) + B_2 \cdot u(t) \\ y(t) &= C \cdot x(t) + D \cdot u(t) \end{aligned} \quad (9)$$

where $[A]_{8 \times 8}$ is the state matrix, $[B_1]_{8 \times 2}$ is the input matrix for perturbations signs, $[B_2]_{8 \times 2}$ is the input matrix for control signs, $[C]_{2 \times 8}$ is the output matrix for states signs, and $[D]_{2 \times 2}$ is the output matrix for control input signs. The state vector (x), the input (“ u ” as control forces, “ w ” as road vertical velocities) and output (“ y ” – bounce and pitch accelerations) vectors are shown in Eq. (10), respectively:

$$\begin{aligned} x &= [x_{A01}, x_{B01}, x_{A12}, x_{B12}, v_{A1}, v_{B1}, v_G, \omega_G]^T \\ u &= [f_A, f_B]^T; w = [v_{A0}, v_{B0}]^T; y = [\ddot{x}_G, \ddot{\theta}_G]^T \end{aligned} \quad (10)$$

This system was analyzed from the point of view of control techniques, and the conclusions are that this system is stable, controllable and observable, so we have good conditions for control design.

For passive situation, the values b_{A12} and b_{B12} are respectively 1750 Ns/m and 2250 Ns/m and the system frequency response for road perturbations is as shown in Fig. (2). On the other hand, for active (or semi-active) application, these dampers will be replaced by actuators (responsible for f_A and f_B forces), which have a residual damping rate around 400Ns/m, what is called "soft-damping".

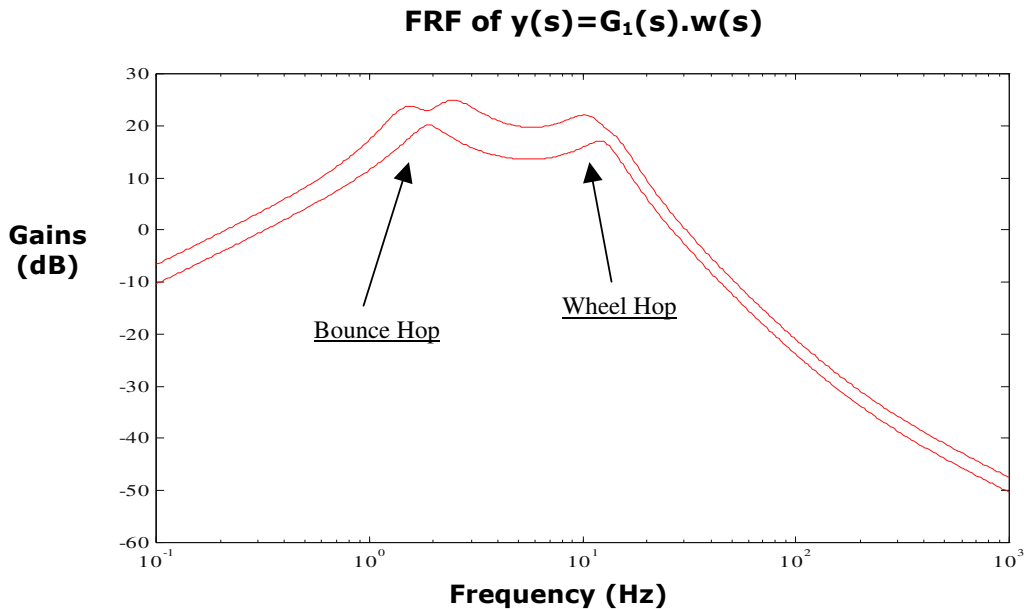


Figure 2 – Frequency Response Function (FRF) of $y(s)=G_1(s)w(s)$ [singular values (dB) versus frequency (Hz)]

As we can see in the above diagram, Fig. (2), the gain between measured accelerations and road vertical velocities can achieve 20dB at the resonant frequencies. The two resonant points represent the two major vibration modes: bounce and wheel hopping respectively.

3. Magneto-Rheological Device

A Magneto-Rheological (MR) damper is very similar to the traditional damper as shown in Spencer and Dyke (1996). The difference is that the first one use a magneto-rheological fluid inside, which typically consists of micron sized, magnetically polarizable particles dispersed in a carrier medium such as mineral or silicone oil. When a magnetic field is applied to the fluids, particle chains form, and fluid becomes a semi-solid, exhibiting plastic behavior, and so changing the flow properties of the fluid. Transitions to rheological equilibrium can be achieved in a few milliseconds, providing devices with high bandwidth. Thus a MR damper could be build using a traditional damper body, using magnetic valves able to act over the MR fluid property. The peak power required to fluid control is less than 10 watts, which could allow the damper to be operated continuously for more then an hour on a small camera battery. A schematic drawing of a MR damper is shown in Fig (3).

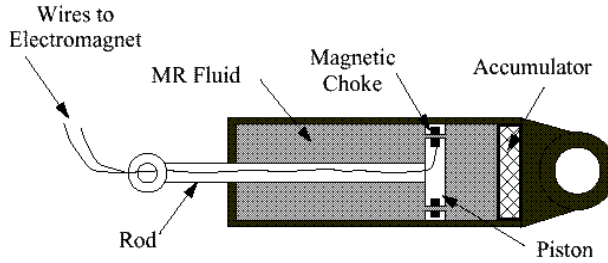


Figure 3 – Magnet-Rheological damper

Built this way these dampers start to have the property of generating forces in the opposite sense to the movement of its piston that are related to two aspects: one of them is the same of the traditional dampers that it corresponds to a viscous friction whose generated force is proportional to the speed of the piston. The other aspect is related to the effect magneto-rheological in the valves of adjustable magnetic field, whose force correspondent doesn't just depend on the speed, but also on the electric current (or indirectly of the electric tension) applied to the solenoid of the valve. And, in this case, the dependence of the speed is not more linear as in the viscous friction.

For the study presented in this work, a simplified model of this device was used. The "histereses" effect, as shown in Fig. (4), right graph and light blue curves, was not considered in the model. The simplified model behavior is also shown in Fig. (4), right graph, but in black colored curves. Although the "histereses" feature has been neglected, its effect on Force versus Displacement relationship is insignificant, as shown in Fig. (4), left graph.

The mathematical representation of this model is given for:

$$f = b \cdot \Delta v + \alpha(\Delta v) \cdot \eta \cdot i \quad (11)$$

where 'b' it is the coefficient of linear friction that in this study was considered 400Ns/m (soft-damping); ' Δv ' is the difference of the velocities in each extremity of the MR Damper; ' η ' is the constant that relates electric current and force, ' i ' it is the electric current in the solenoid of the valves; and finally, ' α ' is a constant that depends on the sense of the velocity, once the forces only show in opposition to the movement, and it acts in the following way:

$$\alpha(\Delta v) = \begin{cases} 1, \dots \text{if } \Delta v > 0 \\ -1, \dots \text{if } \Delta v < 0 \\ 0, \dots \text{if } \Delta v = 0 \end{cases} \quad (12)$$

In addition, two other limitations were adopted in this model: the first one is that the maximum dissipative force of the MR damper is 2000 Ns/m, and the second one is that a first order time delay (around 5ms) was adopted in order to be representative of the time necessary to the MR fluid respond to the electric excitation, added to some delay caused by the electronic circuit of excitation.

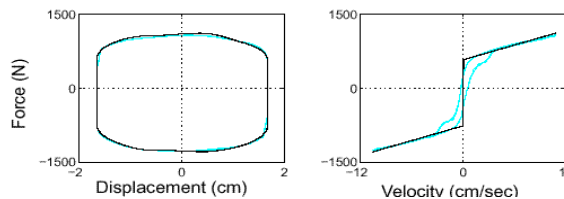


Figure 4 – Characteristics curves of Magneto-Rheological damping used in the simulations.

4. Design of Controller

The main goal of the controller that we will design is to act in the plant in order to reduce the perturbation effects (road) in the vehicle body, and consequentially in the driver and in the passenger bodies. Thus the block diagram of the plant should have two inputs, one regarding road perturbations and other regarding control signals, and one output regarding the accelerations measured and used for control feedback. In the Fig (5) we can see a generic block diagram for a control system.

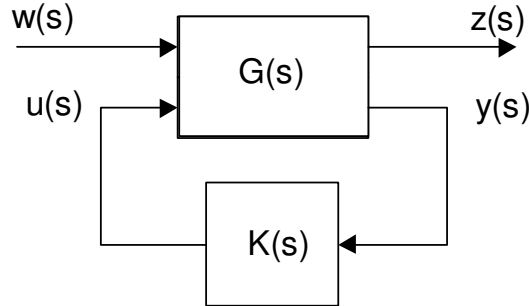


Figure 5 – Generic structure of Plant and Controller

Considering the above diagram we have the following equations in frequency domain:

$$G(s) = \begin{bmatrix} G_{11}(s) & G_{12}(s) \\ G_{21}(s) & G_{22}(s) \end{bmatrix} \quad (13)$$

$$\begin{cases} z(s) = G_{11}(s) \cdot w(s) + G_{12}(s) \cdot u(s) \\ y(s) = G_{21}(s) \cdot w(s) + G_{22}(s) \cdot u(s) \\ u(s) = K(s) \cdot y(s) \end{cases}$$

On the other hand, the Space State representation is the following:

$$\begin{aligned} \dot{x}(t) &= A \cdot x(t) + B_1 \cdot w(t) + B_2 \cdot u(t) \\ z(t) &= C_1 \cdot x(t) + D_{11} \cdot w(t) + D_{12} \cdot u(t) \\ y(t) &= C_2 \cdot x(t) + D_{21} \cdot w(t) + D_{22} \cdot u(t) \end{aligned} \quad (14)$$

For this work we can do some simplifications such as “y=z”, “D₁=0” and “D₂” could be called “D” only. The effect of this is to reduce the equations above to the following system in frequency domain:

$$G(s) = \begin{bmatrix} G_1(s) & G_2(s) \end{bmatrix}$$

$$\begin{cases} y(s) = G_1(s) \cdot w(s) + G_2(s) \cdot u(s) \\ u(s) = K(s) \cdot y(s) \end{cases} \quad (15)$$

In the Space State the representation is reduced to what we have already shown:

$$\begin{aligned} \dot{x}(t) &= A \cdot x(t) + L \cdot w(t) + B \cdot u(t) \\ y(t) &= C \cdot x(t) + D \cdot u(t) \\ L &= B_1 \\ B &= B_2 \end{aligned} \quad (16)$$

Analyzing first the Matrix of the transfer function: $y(s)=G_2(s) \cdot u(s)$, it is important to observe that all poles and transmission zeros have negative or null real part. In special we have four transmission zeros in the origin of the Complex plane, nothing forbidding the use of the LQG/LTR Robust Control Design technique, though, which have non-minimum phase zeros (those with positive real part) as restriction.

Other important issue is that the open loop gain of the plant is very low, which can difficult the design of the controller. As a matter of fact, as it could be demonstrated, the D plant matrix must be orthogonal for the Looping Transfer Recovery (LTR) procedure to be possible. Because of this we must do the following orthogonalization procedure, shown in Eq. (17), where the only restriction is that D matrix must have full rank:

$$\begin{aligned}
S_u &= ((D^T \cdot D)^{1/2})^{-1} \\
B_n &= B \cdot S_u \\
D_n &= D \cdot S_u
\end{aligned}
\tag{17}$$

The S_u matrix got from this way is applied as a constant Gain matrix put in the input of the plant (actuator). Thus the Controller is designed considering S_u making part of the plant, although, in practice, S_u is a part of Controller block.

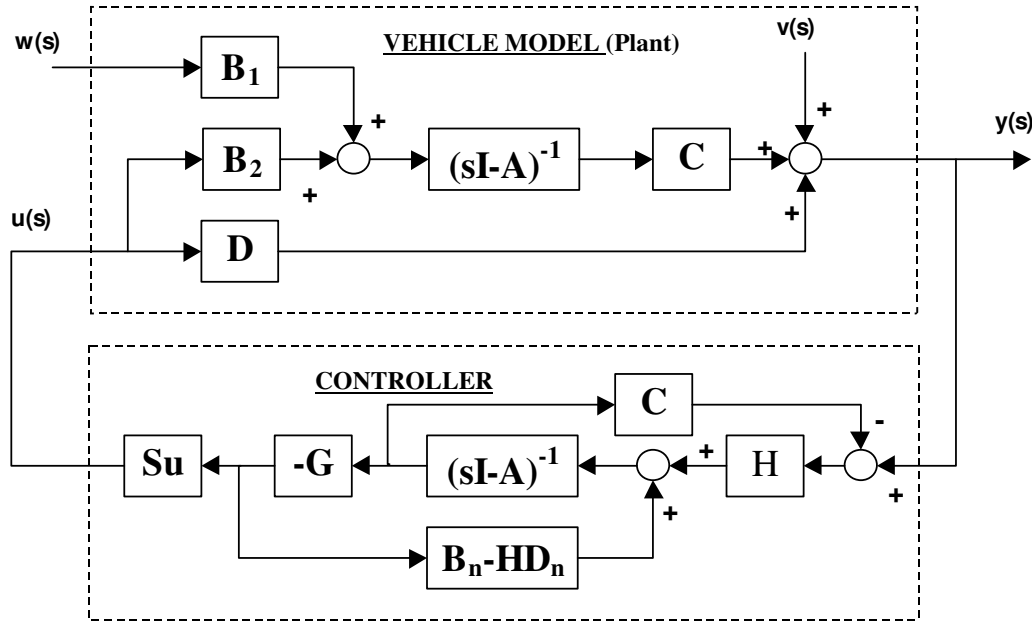


Figure 6 – Block Diagram of the Active Control System

The Fig (6) shows the block diagram of the active control. This diagram considers the particular case (or more general case) of the existence of D matrix in the plant, and also considers S_u matrix as part of the controller. When the D matrix is present we must proceed in the following way for LQG design:

- 1) The feedback of $u(t)$ signal in the Kalman filter input (observer) is not made through “B” matrix only, instead it must be used “B-HD” matrix. In this case were used B_n and D_n because of the normalization.
- 2) In order to find G matrix using LQG method, it must be considered the cross term in the cost function: $2 \cdot (y^* N \cdot u)$.
- 3) To solve this optimization problem, in Eq. (18), the matrixes Q_2 , Q_3 , R_2 and N must be calculated (Eq. (19) to (22)).

$$J = \lim_{T \rightarrow \infty} \int_0^T \{x^T \cdot Q_2 \cdot x + 2 \cdot y^T \cdot N \cdot u + u^T \cdot R_2 \cdot u\} \cdot dt
\tag{18}$$

Thus some calculations are necessary before Riccati equation to be solved:

$$Q_2 = C' Q C \quad \rightarrow \text{Q matrix, the same when it is used in the simple case.} \tag{19}$$

$$R_2 = R + D' Q D \quad \rightarrow \text{new R matrix, considering D matrix.} \tag{20}$$

$$N = C' Q D \quad \rightarrow \text{N matrix for cross-related terms.} \tag{21}$$

$$Q_3 = Q_2 - N R_2^{-1} N' \quad \rightarrow \text{must be Positive semi-defined.} \tag{22}$$

- 4) Afterwards, the Algebraic Riccati Equation must be solved to find X matrix and to calculate the gain matrix G.

$$-X A - A' X - Q_3' Q_3 + X B R_2^{-1} B' X = 0 \quad \rightarrow X = \text{ARE}(A, B R_2^{-1} B', Q_3) \text{ in the Matlab}^\circledast \tag{23}$$

$$G = R_2^{-1} (N' + B' X) \quad \rightarrow \text{new calculation for G considering N matrix.} \tag{24}$$

4.1 Evaluation of Modeling Error

For evaluation of the modeling error it was considered two dynamics that exist in the physical model that was not considered in the mathematical model due to simplifications.

The first of them is a first order delay of the actuators; in other words, it is the reaction time between electronic excitation and effective force generation, which have the following frequency response function:

$$g_{at}(s) = \frac{1}{sT + 1} \quad (25)$$

, where T is a time constant between 2 and 5 ms.

The other dynamics neglected in the model was the modal vibration of the structure of the vehicle that can be obtained through the modal analysis of the structure. Here it was just analyzed the modes with low frequency (close to the Controller bandwidth operation) and with biggest power (that can really influence in the control performance).

The difficulty of these dynamic modeling is more related to determine its damping coefficient, once the frequency is easier to obtain with reasonable precision using techniques such as finite elements analysis and experimental modal analysis.

Thus the representative frequency response function of those vibration modes unknown is given by:

$$g_{mod1} = \frac{\omega^2}{s^2 + 2 \cdot \xi \cdot \omega + \omega^2} \quad \text{where} \rightarrow \begin{cases} 50 \leq \xi \leq 500 \\ \omega = 2\pi f \Rightarrow f = 45\text{Hz} \end{cases} \quad (26)$$

Through the variation of damping coefficient we could get different frequency response function, from the super-damped to sub-damped that has a resonant point around 45 Hz.

The following step was to find the representative function of the modeling error. To build this function was took the worst case of all analyzed function. Afterwards, it was calculated in the following way:

$$\begin{aligned} T_1(j\omega) &= I \cdot g_{at}(j\omega) \\ T_2(j\omega) &= I \cdot g_{mod1}(j\omega) \\ G_N(j\omega) &= C \cdot (j\omega \cdot I - A) \cdot B_2 + D \\ G_R(j\omega) &= T_2(j\omega) \cdot G_N(j\omega) \cdot T_1(j\omega) \\ \varepsilon_M(j\omega) &= (G_R(j\omega) - G_N(j\omega)) \cdot G_N^{-1}(j\omega) \\ e(\omega) &\geq \|\varepsilon_M(j\omega)\| \end{aligned} \quad (27)$$

4.2 Definition of Performance Barriers

As in this control design the function of the Controller is just to minimize the effect of disturbances, we fled a little of the standard form of the barriers definition behavior.

Firstly it was neglected the "Reference Signal Tracking barrier", because there is no reference signal.

In order to define the barrier of "Disturbances Rejection" ($1/\alpha_d$), it was used the results of what would be a disturbance in the exit of the plant due to the characteristic signal of a highway applied as vertical speed in the tires of the vehicle. Thus a white noise (infinite spectrum) was introduced in the plant through a "shaping filter" in such a way that the resulting signal had a PSD (Power Spectrum Density) as close as possible that one of real highway. In this work a 1st order "shaping filter" was used, as the following:

$$F(s) = \frac{1}{s + 2 \cdot \pi \cdot \alpha \cdot v} \quad \text{where} \rightarrow \begin{cases} \alpha = 0.3 & (\text{cycles / meter}) \\ v = 20\text{m/s} & (\text{vehicle velocity}) \end{cases} \quad (28)$$

Note: This "shaping filter" was also used in the simulations, and the white noise applied in shaping filter input was enough to generate a road vertical velocity sign around 0.2m/s RMS value.

Thus the barrier of disturbances rejection ($1/\alpha_d$) was defined as being the frequency response of the composition of the transfer function of the Plant with the transfer function of the "shaping filter."

On the other hand, to identify the barrier of "Sensibility by Plant Variations" ($1/\alpha_s$), first the nominal model of the plant was compared with other with some parameters modified, in order to calculate the modeling error in the frequency response function due to variation of specific parameters. The modified parameters were those affected by the "maximum load" and the "without load" situations of the pickup truck vehicle.

It was observed that the modeling error due to variation of the parameters described above is only significant for a limited range of frequencies, so the interval then between 8 and 12 rad/s was adopted as barrier where each 10% of variation in the model must result at the most 5% of variation of the output, i.e., $\alpha_\delta = 50\%$.

Finally, the barrier of “Measurement Error Rejection” was defined as $\alpha_n = 10\%$, i.e., the output effect measurement noise must be reduced at least 10 times for frequencies above 400Hz. This frequency value was adopted in order to close to the sample frequency, i.e., the frequency in that the measured signal will be sampled from the accelerometer (sensors), because it is the frequency where the most part of the noise will be generated. Besides, as the signal is sampled by a zero order sample-hold, the controller will need to be converted to a discrete domain. This process results in the introduction of non-minimum phase zeros in this frequency range, whose effects must be minimized to avoid problems with LQG/LTR approach, which could result in an unstable controller when the plant model have zeros with positive real part.

All performance barriers are shown in the Fig. (7).

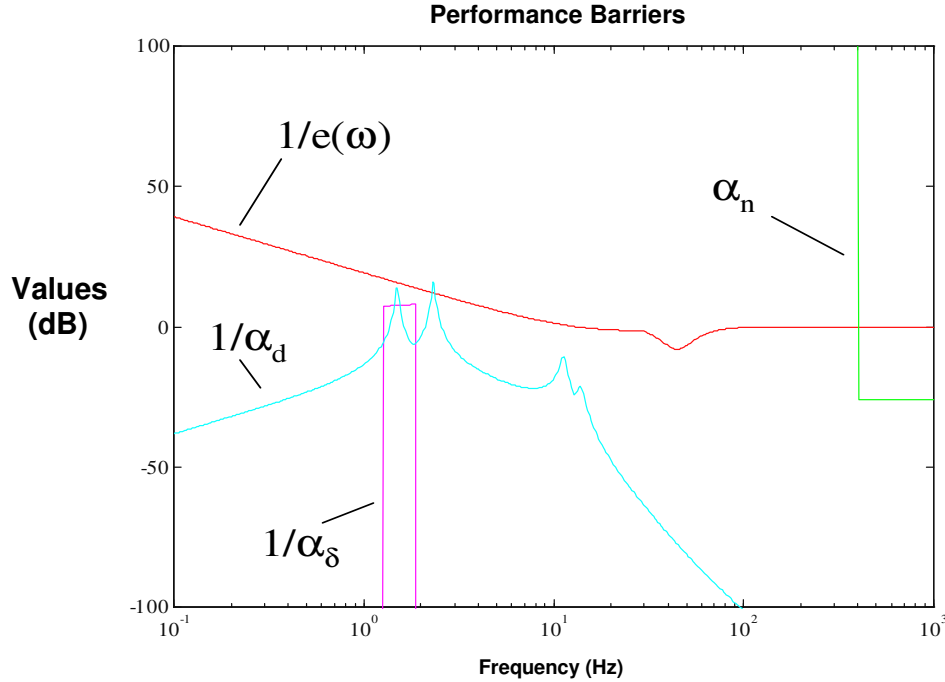


Figure 7 – Performance Barriers.

4.3 LQG/LTR Design Technique

In this work, two LQG/LTR designs were developed with different values for L matrix. Along the application of this approach, comparisons will be made between the two projects, identifying the advantages and disadvantages of each one.

- 1) The first step was choose the L matrix (Gaussian perturbation input matrix) and μ in order to fit the FRF of

$$\frac{1}{\sqrt{\mu}} \sigma_i [C(j\omega \cdot I - A)^{-1} L] \quad (29)$$

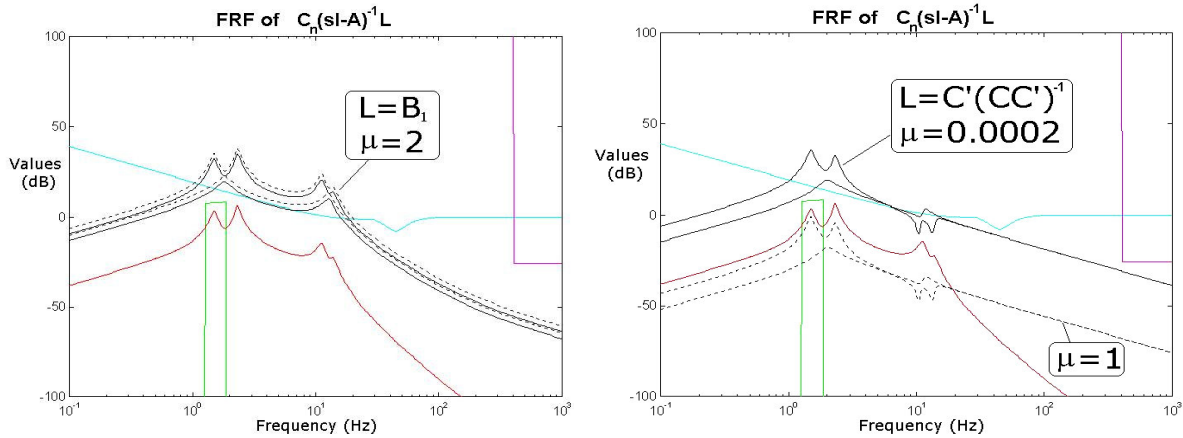
inside the performance barriers, according to Fig (8).

- 2) Calculate H (Kalman filter gain matrix) by solving the following Algebraic Riccati Equation (ARE):

$$A \Sigma + \Sigma A^T + L L^T - \frac{1}{\mu} \Sigma C^T C \Sigma = 0 \quad \Rightarrow \quad H = \frac{1}{\mu} \Sigma C^T \quad (30)$$

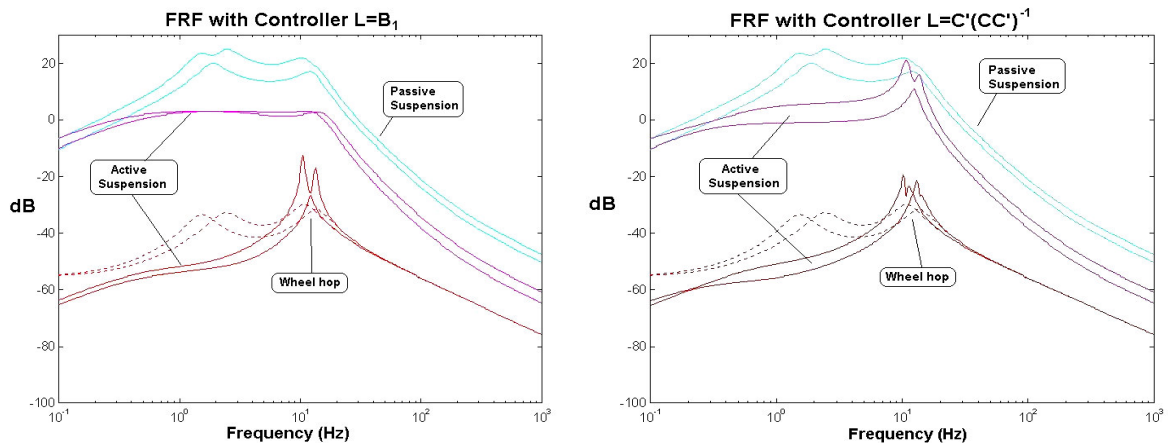
and verify Kalman identity using $G_{KF}(j\omega) = C(j\omega I - A)^{-1} H$.

- 3) Solve the Algebraic Riccati Equation (ARE), as described in the end of the section “4.” of this paper (Eq. (23)), and to find the matrix X (as described a priori).
- 4) Through the FRF of “ $G_N(j\omega)K(j\omega) = (C(j\omega I - A)^{-1} B + D)G(j\omega I - A + B G + H C - H D G)^{-1} H$ ”, it is possible to verify that the condition of robustness of stability was satisfactory, as shown in the Fig.(8).



Figures 8 – Adjust of Transfer Function “ $G_N(j\omega)K(j\omega)$ ” inside the barriers. **Note:** dashed line means $\mu = 1$

- 5) To verify the comfort performance of the Controller designed, should be used the answer in $y(s)=G_1(s)w(s)$. Comparing it with the result of the passive suspension (blue curves), we verified a better performance of the Controller based on “ $L=B_1$ ”, according to Fig. (9), left graph, where we can see a reduction of the disturbance along the full range of work of the suspension (violet curve). In the Fig. (9), right graph, we have the Controller based on “ $L=C'(CC')^{-1}$ ”.
- 6) To verify the safety performance, the frequency response function of tire deflection amount as the result of the road disturbance $w(s)$ was analyzed, as shown in Fig (9) in red curves. It is noticed that the level of resonance of the tires (wheel hopping) is higher in active suspension in relation (continuous curves) to the passive suspension case (dashed curves). In a comparison between the different controller approach, that based on “ $L=B_1$ ” assumption, presents the worst situation.



Figures 9 – Comparison between Frequency Response Function (FRF) with and without controller situation.

5. Results and Conclusions

The simulations were accomplished using the method of numeric integration RK45 (Runge-Kuta 4th and 5th order). As said before, a white noise processed by a “shaping filter” was used to simulate the disturbance signal generated by the road. The values of acceleration of the exit of the plant and the values of deflection of the tires were evaluated as its RMS values. In the simulations, the vehicle speed was 72 km/h, during 20 seconds, what is equivalent to run 400 meters.

Observing the results of the simulations, shown in Tab. (1) on the next page, we get the following conclusions:

- 1) The designed controller got from $L=B_1$ assumption presented the better performance in comfort (reduced RMS accelerations rates), on the other hand, degraded a lot the performance regarding security issue (significant RMS tire decompress rates).
- 2) The Controller designed with $L=C'(CC')^{-1}$ did not present such a good improvement of the comfort, even so its performance was very good against the result of the passive suspension. Regarding the safety aspect, the

performance was better than of the other Controller (based on $L=B_1$), however still worse than the result of the passive suspension.

- 3) The simulation results using the MR Damper (semi-active control) and the same control law of controller designed from $L=C'(CC')^{-1}$ was worse than passive suspension results. It occurred because the optimum control law obtained from LQG/LTR technique do not generate control forces synchronized with relative damper velocities, considering the dissipative forces, which MR Damper is able to generate.
- 4) The solution was obtained changing the weights in cost equation for LQG design. Instead of using the Q_3 matrix (Eq.(11)), we must use " $k \cdot Q_2$ ", where " k " is a constant have chosen in order to improve the importance of some state variables in the optimization cost function, without losing the robustness of the LQG/LTR controller. The results can be seen in the last two lines of Table (1), where this comfort index value is between passive and active suspension performance results. In addition, considering the security issue, the result was better than the others, illustrated by the fact that this was the unique case where rear tire did not lose contact with the ground. Other very important issue is that the maximum deflection of suspension was almost the same that from passive case, what lead us to a situation where is not necessary a new design of suspension geometry.

Table 1 – Simulation Results

Models Simulated	RMS Acceleration Bounce (m/s ²)	RMS Acceleration Pitch (m/s ²)	Frontal Tire RMS decompress (cm)	Rear Tire RMS decompress (cm)	Frontal Tire contact minimum normal force (N)	Rear Tire contact minimum normal force (N)	Front suspension maximum deflection (cm)	Rear suspension maximum deflection (cm)
Passive (without load)	1.0	0.9	0.15	0.20	1517	No contact	2.0	1.8
Passive (with load)	0.8	0.4	0.15	0.23	1643	2677	2.6	3.8
Active ($L=B_1$, $\mu=2$, without load)	0.1	0.1	0.26	0.44	257	No contact	3.9	6.0
Active ($L=B_1$, $\mu=2$, with load)	0.1	0.1	0.25	0.39	628	1032	3.6	6.9
Active ($L=C'(CC')^{-1}$ $\mu=0.0002$, without load)	0.3	0.3	0.20	0.28	677	No contact	4.2	4.8
Active ($L=C'(CC')^{-1}$ $\mu=0.0002$, with load)	0.2	0.2	0.18	0.24	908	2187	4.1	5.5
Semi-Active ($L=C'(CC')^{-1}$ $\mu=0.0002$, without load)	1.2	1.0	0.19	0.27	1027	No contact	2.6	2.2
Semi-Active ($L=C'(CC')^{-1}$ $\mu=0.0002$, with load)	0.7	0.4	0.17	0.22	1503	2852	2.6	2.7
Semi-Active ($L=C'(CC')^{-1}$ $\mu=0.0002$, without load, $Q_3=0.2 \cdot Q_2$)	0.7	0.6	0.14	0.21	1622	3	2.2	2.0
Semi-Active ($L=C'(CC')^{-1}$ $\mu=0.0002$, with load, $Q_3=0.2 \cdot Q_2$)	0.5	0.3	0.15	0.23	1713	2992	2.3	3.1

6. References

- 1) Cruz, José Jaime da,1996, "Controle Robusto Multivariável", Edusp, S. Paulo, Brazil, 163 p.
- 2) Hac', Aleksander; Youn, Iljoong Youn; Chen, Hsien H., "Control of Suspensions for Vehicles With Flexible Bodies - Part I:Active Suspensions and Part II: Semi-active Suspensions", September 1996, Transactions of the ASME, vol.118, pp 508 – 525.
- 3) Inman, Daniel J, 1996, "Engineering Vibration", Prentice Hall, Upper Saddle River, NJ07458, 560 p.
- 4) Ogata, Katsuhiko, 1970, "Engenharia de Controle Moderno", Prentice/Hall, Englewood Cliffs, N.J. USA, 929.
- 5) SAE J1490 Jan87 – "Measurement and presentation of truck ride vibrations".
- 6) Simon, D.E., Ahmadian, M., "An alternative semi-active control method for sport utility vehicles", Proc Instn Mech Engrs Vol 216 Part D: J Automobile Engineering, D12100@IMechE 2002, pp 125 – 139.
- 7) Spencer, B.F., Jr., S.J. Dyke, M.K. Sain and J.D. Carlson, March 10, 1996, "Phenomenological Model of a Magnetorheological Damper", ASCE Journal of Engineering Mechanics.
- 8) Spencer, B.F., Jr., S.J. Dyke, M.K. Sain and J.D. Carlson, June 30 to July 5, 1996, "Seismic Response Reduction Using Magnetorheological Dampers", Proceedings of the IFAC World Congress, San Francisco, CA, USA.
- 9) Tamai, Edilson H., PHD, 1995, 'Estudo do Problema de Controle da Suspensão de Trens de Alta Velocidade Levitados Magneticamente', PHD Tese, PMC FT-891, UNESP-DEM, S. Paulo, Brasil.

7. Copyright Notice

The author is the only responsible for the printed material included in this paper.